

# Axi-symmetric compression of solid cylinders

## Part I *Slow loading conditions*

A. P. SINGH<sup>†</sup>, K. A. PADMANABHAN

*Department of Metallurgical Engineering, Indian Institute of Technology, Madras 600 036, India*

The analytical and experimental methods of determining the compressive yield stress of materials have been reviewed briefly. Using aluminium, EN 24 steel, lead and a tin–lead eutectic alloy, the areas of applicability of the Cook and Larke method (including its modified form for strain-rate sensitive materials) and the ring compression test have been delineated. Under conditions of sliding friction, both the methods give similar values for the coefficient of friction. Under sticking or near-sticking friction conditions, the modified Cook and Larke method is more accurate, because the interpretation of the ring compression test ignores the strain-rate sensitivity of the flow stress. Within the experimental range, the coefficient of friction and the interface friction factor were unaffected by the changes in the strain level, strain rate, grain size and efficacy of lubrication. Under slow loading conditions, the effect of specimen dimensions on the flow stress could be attributed entirely to a change in the frictional contribution. The strain and/or strain-rate hardening behaviour, as well as the grain size dependence of the flow stress of the different materials, were consistent with earlier well-known results.

### 1. Earlier work

For evaluating the true stress–true strain curves of materials, axi-symmetric compression of solid cylinders is often used. In these tests friction is present and this leads to barrelling [1, 2]. But the analysis of many metal-forming processes, e.g. extrusion, requires a knowledge of the compressive yield stress of a material, i.e. which is corrected for friction [3, 4]. A correction for friction can be effected either analytically or experimentally.

For analysing a cold-working process, Coulomb's law  $\tau = \mu N$ , where  $\tau$  is the frictional (shear) stress,  $\mu$  is the coefficient of friction and  $N$  is the normal stress, is often used. While in most analyses  $\mu$  is treated as constant, in reality it depends on a number of variables in a complicated way, e.g. material properties, efficacy of lubrication, rate of sliding at the interface. In hot working, on the other hand, sticking friction is assumed. Here the frictional stress is taken as equal to the shear yield stress of the material in plane strain, again an idealized picture [5, 7].

A barrelling correction, which is analogous to necking correction in tension, is often made. But this calculation is influenced by the specimen dimensions and the lubricant used. Additionally, some questionable assumptions are also involved in the analysis [8–11].

Slip-line field solutions are often inapplicable for axi-symmetric flow problems [12–17].

Early experimental methods of Rummel, Meyer and Nehl and Siebel and Pomp are only of historical significance [18–24]. The methods of Taylor and Quinney [25], Ford [26] and Polakowski [23] are time consuming as they require remachining (which also changes the overall mechanical history of the specimen) and cannot be used when an allotropic transformation is present in the material, e.g. a steel. Moreover, the first two methods employ a lubricant and the compressive yield stress then changes with the lubricant used.

Use of concentric grooves at the ends of a specimen to trap the lubricant may eliminate barrelling [27]. A PTFE (Teflon) sheet of the right thickness, when employed as a lubricant, minimizes both barrelling and bollarding [28, 29].

Compression of specimens of a dumb-bell shape [30] or a reduced gauge section [31] has been considered. Procedures for identifying the sources of error in stress determination have been suggested [32–34].

Körber and Müller [35] and Sachs [36, 37] had anticipated the Cook and Larke technique [2], in which specimens of different initial diameter-to-height ratios,  $D_0/H_0$ , are compressed by a fixed amount. The observed stress,  $\sigma_{\text{obs}}$ , is then plotted against the  $D_0/H_0$  values. Extrapolation to  $D_0/H_0 = 0$  gives the compressive yield stress for the given degree of compression. Polakowski's criticism [23] that the compressive yield stress predicted by this method is

<sup>†</sup> Present address: Research and Development Centre for Iron and Steel, Steel Authority of India Limited, Ranchi 834 002, India.

less than that obtained from other procedures is not valid, because he used the maximum diameter of the barrel instead of the diameter of an equivalent cylinder, while calculating the stress. (A modified form of this test is due to Watts and Ford [38], in which the percentage reduction is plotted against the  $D_o/H_o$  ratio to obtain the percentage compression for the frictionless case by extrapolation to  $D_o/H_o = 0$ .)

Ideally, for obtaining the compressive yield stress at high strain levels, material subjected to homogeneous strain by an amount slightly less than the required value should be used while making specimens of different  $D_o/H_o$  values. The specimens should then be compressed by the required (small) amount and the compressive yield stress at this strain determined by the Cook and Larke procedure.

But the Cook and Larke plots [2, 9] reveal that up to 60%–70% reduction in height the  $\sigma_{obs}-(D_o/H_o)$  relation is linear. (Beyond this level, friction could modify the stress state and introduce non-linearity.) Hill [14] pointed out that as long as the  $\sigma_{obs}-(D_o/H_o)$  relationship is linear, extrapolation to  $D_o/H_o = 0$  will give the compressive yield stress at the corresponding strain. Thus, in this region uniaxial compression itself may be regarded as a way of imparting the required homogeneous strain [9, 39].

It is safe to note at this stage that notwithstanding its simplicity and sound scientific basis, the Cook and Larke method is popular mostly among British-trained scientists. In fact, Richardson *et al.* [40] have advocated the use of this technique even at strains where the  $\sigma_{obs}-(D_o/H_o)$  relationship is non-linear.

Because in a modern testing machine a continuous record of the force and crosshead/tool displacement can be obtained, Padmanabhan and Davies [39] have suggested that with one set of specimens of different initial diameter-to-height ratios compression could be continued up to those strain levels at which the end effects introduce non-linearity (usually at 60%–70% reduction in height). Then, at fixed strains, e.g. 10%, 20%, 50% reduction in height,  $\sigma_{obs}-(D/H)$  plots may be drawn to obtain the compressive yield stress by extrapolation to  $D/H = 0$ . ( $\sigma_{obs}-(D_o/H_o)$  plots and  $\sigma_{obs}-(D/H)$  plots are equivalent [39, 40]; here  $H$  is the instantaneous height of the specimen estimated from the tool movement and  $D$  is the current diameter of the (equivalent) cylinder calculated from a constant specimen volume.)

If the material is strain-rate sensitive, e.g. a superplastic alloy, by a proper choice of tool velocities/crosshead speeds both the strain and strain rate should be kept constant simultaneously, before making the  $\sigma_{obs}-(D/H)$  plots [39].

It is seen from theory that under conditions of Coulomb friction [1]

$$\sigma_{obs} = \sigma_o [1 + (\mu/3)(D/H)] \quad (1)$$

where  $\sigma_o$  is the compressive yield stress at the given strain. Alternatively, particularly under conditions of hot working, a constant friction factor,  $m^*$ , is used. Then

$$\sigma_{obs} = \sigma_o [1 + (m^*/3 \times 3^{1/2})(D/H)] \quad (2)$$

where  $m^*$  (the interfacial shear stress/shear yield stress) may vary from zero (frictionless condition) to 1 (sticking friction) [41].

The coefficient of friction over a wide range of strain, strain rate, temperature and lubrication conditions may also be evaluated from a ring compression test [42]. An initially used ring geometry [43, 44] of outer diameter (o.d.): inner diameter (i.d.): height 6:3:2 appears to have become an unofficial standard. The analysis assumes a constant coefficient of friction and considers the changes in the geometry of the specimen [42, 45–48]. Bulging has also been taken into account [43, 49–52]. In addition, it is possible to determine  $m^*$  from this test [53–56]. This method is considered to be one of the best for determining the interfacial friction coefficient at both room and elevated temperatures.

Plastic properties of commercial aluminium [53, 57], lead [58–62] and some materials of high strain-rate sensitivity [63–68] have been determined in compression.

The loading rate is important; three ranges have been identified, slow loading, rapid loading and instantaneous loading conditions [69].

## 2. Scope of the present study

In Part I of this work, room-temperature axi-symmetric compression under slow loading conditions of aluminium, EN 24 steel, lead and a tin–lead eutectic alloy is considered. The tests correspond to cold working for aluminium and steel but hot working in the case of lead and the lead–tin alloy.

The coefficient of friction and the interfacial friction factor were determined using both the Cook and Larke method, described above, and the ring compression test. The results were compared with a view to identifying the range of applicability of each procedure.

The compressive yield stress–true strain plots generated under slow loading conditions represent approximately isothermal response of a material. Material subjected to rapid loading, on the other hand, experiences “adiabatic” heating due to the plastic work of deformation. It would be interesting to see which of the above methods is applicable under rapid loading conditions and if the curves pertaining to the two ranges can be made to superimpose by incorporating suitable strain rate and temperature corrections. This problem is considered in Part II [70].

## 3. Experimental procedure

### 3.1. Specimens for Cook and Larke tests

A slab of commercial aluminium of composition (wt %) Fe 0.18, Si 0.12, Al balance, was melted in a crucible furnace and cast into bars of 25.40 mm diameter. The bars were forged at room temperature to a diameter of 12.70 mm. Cylindrical specimens of a constant diameter of 10.16 mm and different  $D_o/H_o$  ratios of 1.00, 0.80 and 0.67 were machined from the forged bars. Batches of specimens were annealed in a fused salt bath at 473, 573, and 673 K for 3.6 ks

to obtain two-dimensional grain sizes of  $50 \pm 0.2 \mu\text{m}$ ,  $62 \pm 0.3 \mu\text{m}$  and  $73 \pm 0.2 \mu\text{m}$ , respectively.

EN 24 steel had a composition (wt %) C 0.34, Mn 0.49, Cr 0.94, Ni 1.80, S 0.01 and P 0.02. Rods of diameter 25.40 mm were machined to obtain cylindrical specimens of dimensions identical to those made from aluminium. The specimens having a two-dimensional grain size of  $10 \pm 0.4 \mu\text{m}$  were tested in the as-received condition.

A slab of commercial lead of 99.9% purity (with traces of Cu, Zn, Fe and Ag) was melted in a crucible furnace and cast into bars of 25.40 mm diameter. Following room-temperature (hot) forging to a diameter of 12.70 mm, cylindrical specimens of a constant diameter of 10.16 mm and varying  $D_0/H_0$  ratios of 1.33, 1.00 and 0.67 were machined. A two-dimensional grain size of  $79 \pm 0.4 \mu\text{m}$  was developed in the specimens by heat treating them for 3.6 ks in boiling water maintained at 373 K.

A Sn-38 wt % Pb eutectic alloy was melted in a resistance furnace and cast into bars of 25.40 mm diameter. After (hot) forging at room temperature to rods of diameter 12.70 mm, cylindrical specimens identical to those made of lead were prepared. By heat treating different batches for 0.9 ks in an oil bath at 373, 403 and 423 K, two-dimensional grain sizes of  $6.2 \pm 0.1 \mu\text{m}$ ,  $7.1 \pm 0.2 \mu\text{m}$  and  $8.3 \pm 0.2 \mu\text{m}$  were obtained.

### 3.2. Ring compression test specimens

As before, commercial aluminium, commercial lead and the tin-lead eutectic alloy were melted and cast into bars of 50.80 mm diameter. Following room-temperature forging to a diameter of 25.40 mm, ring compression specimens of dimensions 19.05 mm o.d., 9.50 mm i.d. and 6.35 mm height were made. The heat treatments described earlier were used to obtain the grain sizes recorded above for the three materials. Identical ring compression specimens were also made out of the EN 24 steel rod (in the as-received condition).

### 3.3. Compression testing

On account of its higher load requirement EN 24 steel specimens were compressed on a 60 tonne universal testing machine. The non-ferrous specimens, on the other hand, were compressed on a 5 tonne Instron universal testing machine. While plotting the  $\sigma_{\text{obs}}-(D/H)$  relationship, the strain was kept constant in the case of Al and EN 24 steel (cold working). In the case of lead and the tin-lead alloy specimens (hot working/superplasticity) both strain and strain rate were maintained constant simultaneously by suitably adjusting the crosshead speeds. The tests were performed in the lubricated (a general-purpose lithium base grease was used) as well as the unlubricated conditions.  $\mu$  and  $m^*$  were obtained from Equations 1 and 2, respectively. The compressive yield stress,  $\sigma_0$ , -true strain curves were derived following the modified Cook and Larke procedure outlined in Section 1.

The initial strain rates,  $\dot{\epsilon}_0$ , were  $6 \times 10^{-3} \text{ s}^{-1}$  for the steel;  $8.2 \times 10^{-4}$ ,  $8.2 \times 10^{-3}$  and  $8.2 \times 10^{-2} \text{ s}^{-1}$  for Al;  $1.09 \times 10^{-4}$ ,  $1.09 \times 10^{-3}$  and  $1.09 \times 10^{-2} \text{ s}^{-1}$  for Pb and the Sn-Pb alloy. For the ring compression tests also, the universal testing machine and the Instron machine were used for EN 24 steel and the non-ferrous materials, respectively. The initial strain rates were identical to those used for compressing the solid cylinders. The percentage compression varied between 10 and 50%. For each material, the percentage change in the internal diameter of the ring was plotted against the percentage reduction in height.

## 4. Results

In lead and the tin-lead alloy,  $\sigma_{\text{obs}}$  went through an early maximum with strain, before attaining a "steady state" in which its strain dependence was small. (Such behaviour is typical of hot working and superplasticity [9, 39].) While analysing the present results, only data pertaining to the "steady state" were used. The stress maximum was not present in case of aluminium and EN 24 steel. Two examples of the  $\sigma_{\text{obs}}-(D/H)$  relation are presented in Fig. 1a (aluminium, cold working) and Fig. 1b (the tin-lead alloy, hot working/superplasticity).

From plots similar to the above and Equation 1, the compressive yield stress,  $\sigma_0$ , at a fixed strain was determined as the intercept on the Y-axis. Using this value, the slope of the line and Equation 1,  $\mu$  was calculated. For aluminium and EN 24 steel at all strains,  $\mu$  equalled 0.15. In aluminium this value was also independent of strain rate and grain size.

For lead and the tin-lead alloy, in addition to  $\mu$ ,  $m^*$  was also calculated using Equation 2. In lead, at all strain rates,  $\mu$  equalled 0.54 and  $m^*$  was 0.90. In the tin-lead alloy for strain rates of  $1.09 \times 10^{-4}$ ,  $1.09 \times 10^{-3}$  and  $1.09 \times 10^{-2} \text{ s}^{-1}$ , the values of  $\mu$  were 0.58, 0.54 and 0.48, respectively. The corresponding values of  $m^*$  were 1.00, 0.94 and 0.80. Grain size had no effect on the values of  $\mu$  and  $m^*$ .

For the four materials, from the intercepts on the Y-axis for different true strains,  $\epsilon_t$  (in plots similar to Fig. 1a and b), the  $\sigma_0-\epsilon_t$  curves corresponding to different experimental conditions were derived. Examples concerning three materials are given in Fig. 1c and d, which also display the  $\sigma_{\text{obs}}-\epsilon_t$  relationship for different  $D/H$  ratios (uncorrected for friction).

The  $\sigma_0-\epsilon_t$  relationship for the four materials at different strain rates and grain sizes are given in Table Ia-d. The results of the ring compression tests under different experimental conditions for the four materials are presented in Fig. 2.  $\mu$  was determined by comparing these curves with the calibration charts of Male and Cockroft [42];  $m^*$  (for lead and the tin-lead alloy) by comparison with the charts given by Male and Depierre [54].

For aluminium and the steel,  $\mu$  was 0.15 at all strains (both materials), strain rates and grain sizes (aluminium). For lead, both  $\mu$  and  $m^*$  were independent of strain rate and had values of 0.22 and 0.70, respectively. In the tin-lead alloy,  $\mu$  and  $m^*$  were 0.25

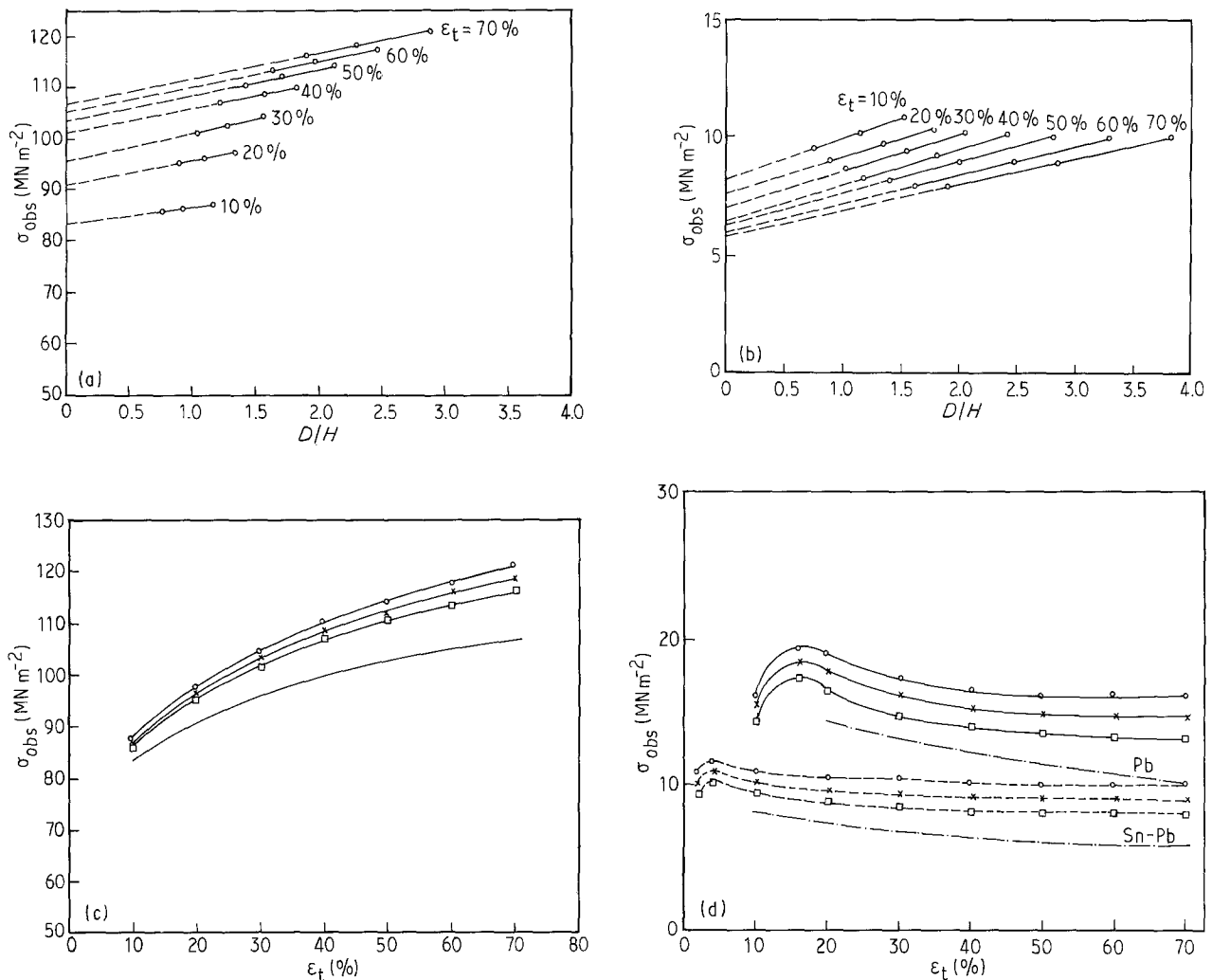


Figure 1 (a, b) Observed true compressive stress,  $\sigma_{obs}$ -( $D/H$ ) relationship at room temperature for different percentage true strains,  $\epsilon_t$ . (a) Commercial aluminium, grain size 50  $\mu\text{m}$ , initial strain rate =  $8.2 \times 10^{-4} \text{ s}^{-1}$ . (b) Tin-lead alloy, grain size 6.2  $\mu\text{m}$ , initial strain rate =  $1.09 \times 10^{-4} \text{ s}^{-1}$ . (c, d)  $\sigma_{obs}$ - $\epsilon_t$  relation at room temperature for different  $D_0/H_0$  values. (c) Commercial aluminium, grain size 50  $\mu\text{m}$ , initial strain rate =  $8.2 \times 10^{-4} \text{ s}^{-1}$ ;  $D_0/H_0$ : (O) 1.00, (x) 0.80, ( $\square$ ) 0.67. frictionless; (—). (d) Lead,  $\dot{\epsilon}_0 = 1.09 \times 10^{-3} \text{ s}^{-1}$ , grain size =  $79 \pm 0.4 \mu\text{m}$ ; (---) the tin-lead alloy,  $\dot{\epsilon}_0 = 1.09 \times 10^{-4} \text{ s}^{-1}$ , grain size =  $6.2 \pm 0.1 \mu\text{m}$ ;  $D_0/H_0$ : (O) 1.33, (x) 1.00, ( $\square$ ) 0.67; (---) frictionless.

and 0.80, respectively. These values were also independent of strain rate and grain size.

In the case of aluminium, the use of a lubricant (a lithium-base general-purpose grease) decreased  $\sigma_{obs}$  at all strains, strains rates and grain sizes by about 5%. But  $\mu$ , determined by both the Cook and Larke and ring compression tests, remained unaffected. In lead and the tin-lead alloy, the use of a lubricant neither decreased  $\sigma_{obs}$  nor altered the values of  $\mu$  and  $m^*$ .

The lead and the tin-lead alloy specimens exhibited some strain softening, which could have been due to grain refinement accompanying the plastic deformation. However, no experimental verification of this idea was made. In the case of aluminium and EN 24 steel the strain hardening index,  $n$ , was calculated in the usual manner using the relation  $\sigma_0 \propto \epsilon_t^n$ . For aluminium,  $n$  was independent of strain rate and had values of 0.13, 0.14 and 0.16 corresponding to grain sizes of 50, 62 and 73  $\mu\text{m}$ , respectively. For the steel,  $n$  was equal to 0.13.

In aluminium, at all strains and strain rates, the relationship  $\sigma_0-d^{-1/2}$  was linear, which verified the Hall-Petch equation in the limited range of grain sizes used in the present experiments. Fig. 3 is an example.

In the tin-lead alloy, which is superplastic at the lower strain rates [39],  $\sigma_0 \propto d^a$ . From the  $\ln \sigma_0$ - $\ln d$  plots,  $a$  was evaluated as 0.9, 0.7 and 0.3 corresponding to the initial strain rates of  $1.09 \times 10^{-4}$ ,  $1.09 \times 10^{-3}$  and  $1.09 \times 10^{-2} \text{ s}^{-1}$  and was unaffected by the strain level. Fig. 4 is one such plot.

The strain-rate sensitivity index,  $m$ , was evaluated as the slope of  $\ln \sigma_0$ - $\ln \dot{\epsilon}_0$  plots [39] for aluminium, lead and the tin-lead alloy. In all cases,  $m$  was independent of the strain level. For aluminium,  $m$  was 0.03 at all three grain sizes. For lead,  $m$  was equal to 0.16 at a grain size of 79  $\mu\text{m}$ . In the tin-lead alloy,  $m$  equalled 0.36, 0.34 and 0.33 corresponding to grain sizes of 6.2, 7.1 and 8.3  $\mu\text{m}$ , respectively. Fig. 5 presents an example in the form of results for the tin-lead alloy.

## 5. Discussion

For aluminium and EN 24 steel, both the Cook and Larke method and the ring compression test gave identical values of  $\mu$ . Thus, either method can be used successfully to derive the compressive yield stress in cold working (up to a maximum true strain of about 70%).

TABLE I Compressive yield stress at different true strains (a) Commercial aluminium, various initial strain rates and grain sizes

| Grain size ( $\mu\text{m}$ ) | Initial strain rate ( $\text{s}^{-1}$ ) | Compressive yield stress ( $\text{MN m}^{-2}$ ) at true strain (%) of |      |       |       |       |       |       |
|------------------------------|---|---|------|-------|-------|-------|-------|-------|
|                              |   | 10  | 20   | 30    | 40    | 50    | 60    | 70    |
| $50 \pm 0.2$                 | $8.2 \times 10^{-4}$                    | 83.0  | 91.0 | 93.0  | 101.0 | 103.5 | 105.0 | 106.5 |
|                              | $8.2 \times 10^{-3}$                    | 87.0  | 92.0 | 96.5  | 101.0 | 104.0 | 106.0 | 108.0 |
|                              | $8.2 \times 10^{-2}$                    | 90.0  | 99.0 | 102.0 | 106.0 | 108.0 | 110.0 | 112.0 |
| $62 \pm 0.3$                 | $8.2 \times 10^{-4}$                    | 72.0  | 81.0 | 85.0  | 88.0  | 90.0  | 91.0  | 92.5  |
|                              | $8.2 \times 10^{-3}$                    | 73.5  | 86.0 | 90.0  | 94.5  | 98.0  | 100.0 | 101.5 |
|                              | $8.2 \times 10^{-2}$                    | 73.5  | 86.0 | 91.0  | 96.5  | 101.0 | 104.0 | 107.5 |
| $73 \pm 0.2$                 | $8.2 \times 10^{-4}$                    | 61.0  | 72.5 | 79.5  | 84.0  | 87.0  | 89.0  | 91.5  |
|                              | $8.2 \times 10^{-3}$                    | 61.0  | 76.0 | 83.0  | 91.0  | 92.0  | 95.0  | 97.5  |
|                              | $8.2 \times 10^{-2}$                    | 73.5  | 83.0 | 91.0  | 95.0  | 100.0 | 102.0 | 104.0 |

(b) EN 24 steel, initial strain rate  $6 \times 10^{-3} \text{ s}^{-1}$ , grain size =  $10 \pm 0.4 \mu\text{m}$

| Compressive yield stress ( $\text{MN m}^{-2}$ ) | True compressive strain (%) |       |       |        |        |        |        |
|---|-----------------------------|-------|-------|--------|--------|--------|--------|
|   | 10                          | 20    | 30    | 40     | 50     | 60     | 70     |
|   | 790.0                       | 932.0 | 975.0 | 1020.0 | 1035.0 | 1043.0 | 1048.0 |

(c) Commercial lead, various initial strain rates, grain size =  $79 \pm 0.4 \mu\text{m}$

| Initial strain rate ( $\text{s}^{-1}$ ) | Compressive yield stress ( $\text{MN m}^{-2}$ ) at true strain (%) of |      |      |      |      |      |
|---|---|------|------|------|------|------|
|   | 20  | 30   | 40   | 50   | 60   | 70   |
| $1.09 \times 10^{-4}$                   | 9.2   | 8.7  | 8.2  | 8.1  | 7.6  | 7.2  |
| $1.09 \times 10^{-3}$                   | 14.2  | 13.2 | 12.0 | 11.4 | 10.8 | 10.0 |
| $1.09 \times 10^{-2}$                   | 19.2  | 17.4 | 16.0 | 15.6 | 15.4 | 14.8 |

(d) Tin-lead eutectic alloy, various initial strain rates and grain sizes

| Grain size ( $\mu\text{m}$ ) | Initial strain rate ( $\text{s}^{-1}$ ) | Compressive yield stress ( $\text{MN m}^{-2}$ ) at true strain (%) of |      |      |      |      |      |      |
|------------------------------|---|---|------|------|------|------|------|------|
|                              |   | 10  | 20   | 30   | 40   | 50   | 60   | 70   |
| $6.2 \pm 0.1$                | $1.09 \times 10^{-4}$                   | 8.1   | 7.5  | 6.9  | 6.4  | 6.2  | 5.9  | 5.8  |
|                              | $1.09 \times 10^{-3}$                   | 19.5  | 18.5 | 17.0 | 15.6 | 15.2 | 14.5 | 14.0 |
|                              | $1.09 \times 10^{-2}$                   | 38.0  | 36.0 | 34.3 | 33.0 | 32.3 | 31.7 | 31.0 |
| $7.1 \pm 0.2$                | $1.09 \times 10^{-4}$                   | 8.8   | 8.2  | 7.9  | 7.7  | 7.3  | 7.1  | 6.7  |
|                              | $1.09 \times 10^{-3}$                   | 22.0  | 20.8 | 19.3 | 18.3 | 17.3 | 16.0 | 15.0 |
|                              | $1.09 \times 10^{-2}$                   | 39.4  | 38.0 | 36.0 | 34.3 | 33.3 | 32.7 | 32.3 |
| $8.3 \pm 0.2$                | $1.09 \times 10^{-4}$                   | 11.0  | 9.8  | 9.3  | 8.5  | 7.9  | 7.7  | 7.2  |
|                              | $1.09 \times 10^{-3}$                   | 22.8  | 20.3 | 20.0 | 19.3 | 18.2 | 17.2 | 15.8 |

For hot working and superplasticity (lead and the tin-lead alloy),  $\mu$  and  $m^*$  values obtained from the modified Cook and Larke method were greater than those resulting from the ring compression test. The results from the former procedure should be regarded as more reliable because the ring compression test (which is based on the analysis of Schroeder and Webster (see [42]) ignores the effect of the strain-rate sensitivity of the flow stress (which was strong in both lead and the tin-lead alloy). Moreover, the unevenness of deformation at low loads could have given rise to inaccuracies in the estimation of the change in i.d. with strain.

Under slow loading conditions, a nearly isothermal response is recorded. Then,  $\mu$  is likely to be independent of strain rate and the conditions of lubrication [42], which is what is observed.  $\mu$  also did not change with grain size in both aluminium and the tin-lead

alloy. This is understandable because a change in grain size only changes the hardness (which is directly related to the flow stress) and it is known that hardness has no effect on  $\mu$  [42]. The results have clearly demonstrated the highly strain-rate sensitive nature of deformation in lead and the tin-lead alloy. In these two materials, lubrication had no effect on the values of  $\sigma_{\text{obs}}$ ,  $\mu$  or  $m^*$ . This indicates the presence of an approximately constant frictional stress and near-sticking friction conditions.

## 6. Conclusions

The present work on the axi-symmetric compression of a solid cylinder under slow loading conditions has led to the following conclusions.

1. Under conditions of cold working (aluminium and steel) the effect of specimen dimensions on the

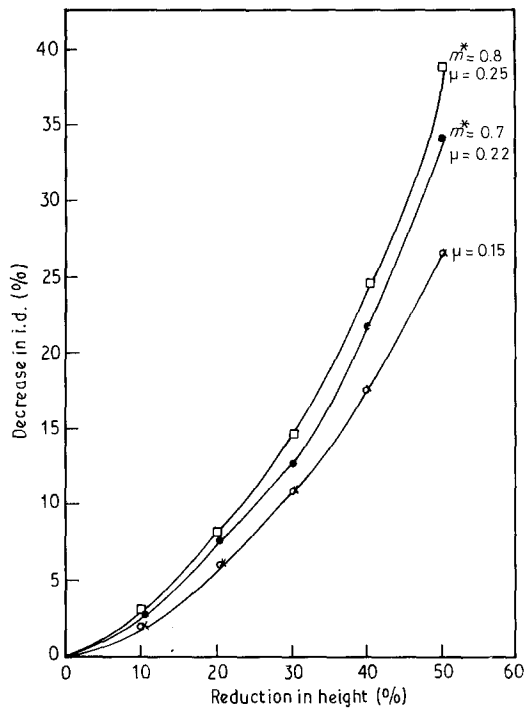


Figure 2 Results of ring compression tests on the four materials: (○) aluminium, (×) EN 24 steel, (●) lead and (□) tin-lead alloy.

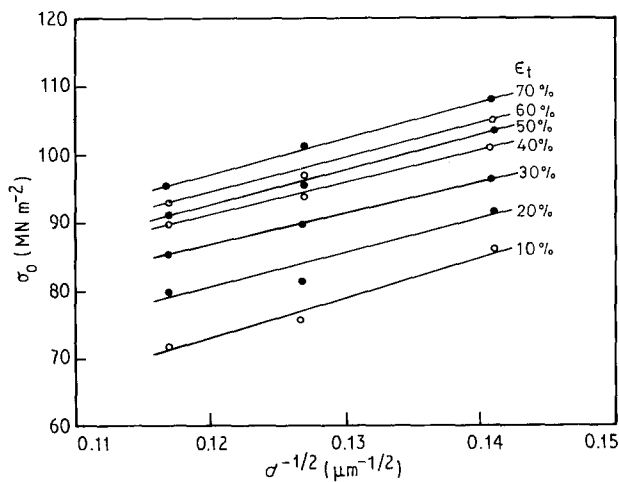


Figure 3 The compressive yield stress,  $\sigma_0-d^{-0.5}$ , where  $d$  is the grain size, relation for different true strains. Commercial aluminium, room temperature. Initial strain rate =  $8.2 \times 10^{-3} \text{ s}^{-1}$ .

flow stress is entirely attributable to friction. The coefficient of friction,  $\mu$ , evaluated by the Cook and Larke method, was equal to that obtained from the ring compression test.

2. In cold working (aluminium), the use of lithium-base grease as a lubricant decreased the flow stress by about 5% (sliding friction). But this lubricant had no effect on the flow stress under conditions of hot working/superplasticity (lead and the tin-lead alloy) (near-sticking friction).

3. Within the experimental range, under conditions of both cold working and hot working/superplasticity, the value of  $\mu$  remained unchanged with the changes in strain rate, grain size and lubricating conditions.

4. Under conditions of hot working/superplasticity, the values of the interface friction factor,  $m^*$ ,

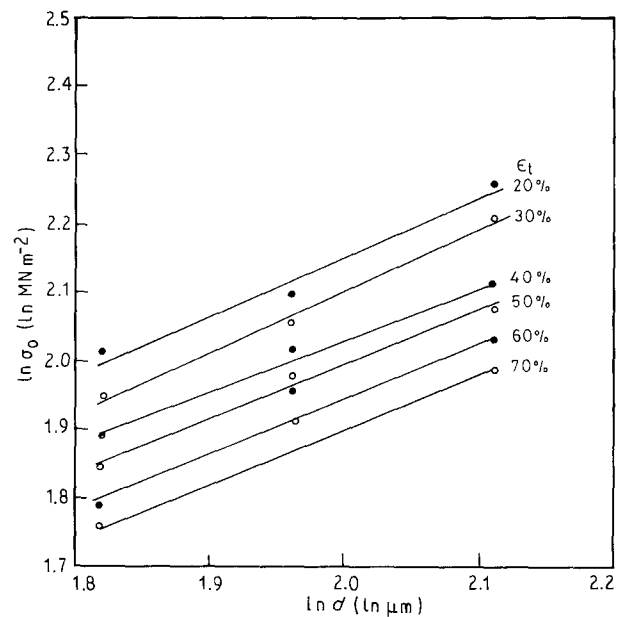


Figure 4  $\text{Ln } \sigma_0 - \text{Ln } d$  relation for different true strains. Tin-lead eutectic alloy, room temperature,  $a = 0.9$ . Initial strain rate =  $1.09 \times 10^{-4} \text{ s}^{-1}$ .

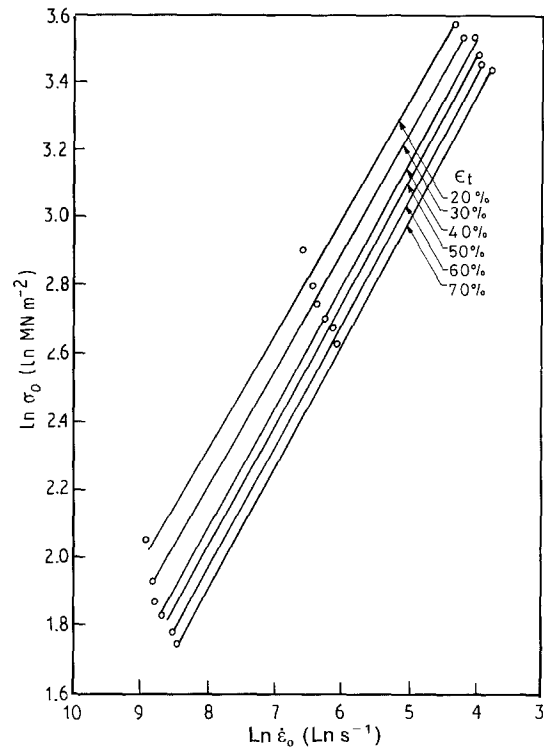


Figure 5  $\text{Ln } \sigma_0 - \text{Ln } \dot{\epsilon}_0$  relation for different true strains. Tin-lead eutectic alloy, grain size  $6.2 \mu\text{m}$ , room temperature,  $m = 0.36$ .

determined from the modified Cook and Larke method [9, 38], were greater than those obtained from the ring compression test. The former values are more dependable because the calibration charts for the ring compression test are derived by neglecting the strain-rate sensitivity of the flow stress.

5. For aluminium (cold working) the strain hardening index,  $n$ , varied between 0.13 and 0.16, but the strain-rate sensitivity index,  $n$ , was low (0.03). In lead and the tin-lead alloy (hot working/superplasticity), on the other hand, some strain softening was present

and  $m$  was large (0.16 for lead and 0.33–0.36 for the tin–lead alloy).

6. In the experimental range, the Hall–Petch relation was obeyed in aluminium but in the tin–lead alloy the compressive yield stress was proportional to  $d^a$ , where  $d$  is the grain size and  $a$  lay between 0.3 and 0.9.

## References

1. G. E. DIETER, "Mechanical Metallurgy", 3rd Edn (McGraw–Hill, New York, 1986) p. 520.
2. M. COOK and E. C. LARKE, *J. Inst. Met.* **71** (1945) 371.
3. P. VENUGOPAL, S. VENKATRAMAN, R. VASUDEVAN and K. A. PADMANABHAN, *J. Mech. Working Technol.* **15** (1987) 357.
4. *Idem.*, *ibid.* **16** (1988) 31.
5. G. T. VAN ROOYEN and W. A. BACKOFEN, *J. Iron Steel Inst.* **186** (1957) 235.
6. O. HOFFMAN and G. SACHS, "Introduction to the Theory of Plasticity for Engineers" (McGraw–Hill, New York, 1953) p. 65.
7. T. A. READ, H. MARKUS and McCaughey, "Fracturing of Metals" (ASM, Metals Park, Ohio, 1948) p. 228.
8. A. NADAI, *Z. Tech. Physik* **5** (1924) 369.
9. K. A. PADMANABHAN, PhD thesis, University of Cambridge (1971).
10. J. K. BANERJEE, *J. Engng Mater. Technol.* **107** (1985) 138.
11. J. K. BANERJEE and G. CARDENAS, *ibid.* **107** (1985) 145.
12. L. PRANDTL, *Z. Angew. Math. Mech.* **3** (1923) 401.
13. A. P. GREEN, *Phil. Mag.* **42** (1951) 900.
14. R. HILL, "The Mathematical Theory of Plasticity" (Oxford University Press, Oxford, 1950) pp. 14, 16, 226–36, 277–8.
15. J. M. ALEXANDER, *J. Mech. Phys. Solids* **3** (1955) 233.
16. J. F. W. BISHOP, *ibid.* **6** (1958) 132.
17. W. SCHROEDER and D. A. WEBSTER, *J. Appl. Mech.* **16** (1949) 289.
18. K. RUMMEL, *Stahl und Eisen* **39** (1919) 237.
19. *Idem.*, *ibid.* **39** (1919) 267.
20. H. MEYER and F. NEHL, *ibid.* **45** (1925) 1961.
21. E. SIEBEL and A. POMP, *Mitteilungen Kaiser Wilhelm Inst. Eisenforschung* **9** (1927) 157.
22. *Idem.*, *ibid.* **10** (1928) 55.
23. N. H. POLAKOWSKI, *J. Iron Steel Inst.* **163** (1949) 250.
24. A. NADAI, "Theory of Flow and Fracture of Solids" (McGraw–Hill, New York, 1950) p. 343.
25. G. I. TAYLOR and H. QUINNEY, *Proc. Roy. Soc. A* **143** (1934) 307.
26. H. FORD, The Iron and Steel Institute (ISI) Special Report no. 39 (Iron and Steel Institute, London, 1947) pp. 21, 23.
27. N. LOIZOU and R. B. SIMS, *J. Mech. Phys. Solids* **1** (1953) 234.
28. G. W. ROWE, "An Introduction to the Principles of Metal Working" (Edward Arnold, London, 1971) p. 280.
29. T. C. HSU, *Mater. Res. Stand.* **9** (1969) 20.
30. K. POHLANDT and W. NESTER, *Wire* **32**(3) (1982) 150.
31. R. COLAS and A. GRINBERG, *Scripta Metall.* **20** (1986) 135.
32. W. NESTER and K. POHLANDT, *Arch. Eisenhüttenw.* **53**(4) (1982) 139.
33. K. POHLANDT and W. NESTER, *Z. Werkstofftech.* **13**(4) (1982) 116.
34. W. REISS and K. POHLANDT, *Exp. Tech.* **10**(1) (1986) 20.
35. F. KÖRBER and A. MÜLLER, *Mitteilungen Kaiser Wilhelm Inst. Eisenforschung* **8** (1926) 194.
36. G. SACHS, *Z. Metallkde* **16** (1924) 55.
37. *Idem.*, *Handbuch Exp. Physik, Akad. Verlag* **5** (1930) 260.
38. A. B. WATTS and H. FORD, *Proc. Inst. Mech. Eng.* **169** (1955) 1141.
39. K. A. PADMANABHAN and G. J. DAVIES, *Met. Sci.* **11** (1977) 177.
40. G. J. RICHARDSON, D. N. HAWKINS and C. M. SELLARS, "Worked Examples in Metal Working" (The Institute of Metals, London, 1985) pp. 6–13.
41. B. AVITZUR, "Metal Forming Processes and Analysis" (McGraw–Hill, New Delhi, 1977) pp. 113, 114.
42. A. T. MALE and M. G. COCKCROFT, *J. Inst. Met.* **93** (1964–65) 38.
43. A. T. MALE, *ibid.* **93** (1964–65) 489.
44. A. T. MALE and M. G. COCKCROFT, *ibid.* **94** (1966) 121.
45. H. KUDO, in "Proceedings of the 5th Japan National Congress for Applied Mechanics" (1955) p. 75.
46. B. AVITZUR, *Israel J. Technol.* **2** (1964) 295.
47. J. B. HAWKYARD and W. JOHNSON, *Int. J. Mech. Sci.* **9** (1967) 163.
48. M. BURGENDORFF, *Ind. Anzeiger* **89** (1967) 799.
49. V. DEPIERRE, F. GURNEY and A. T. MALE, Technical Report no. 37 (Airforce Materials Laboratory, Wright Patterson Air Force Base, Dayton, Ohio, 1972).
50. C. H. LEE and T. ALTAN, *J. Engng Ind. Trans. ASME* **94** (1972) 775.
51. J. Y. LIU, *ibid.* **94** (1972) 1149.
52. G. D. LAHOTI and S. KOBAYASHI, *Int. J. Mech. Sci.* **16** (1974) 521.
53. V. DEPIERRE and A. T. MALE, Technical Report no. 28 (Airforce Materials Laboratory, Wright Patterson Air Force Base, Dayton, Ohio, 1969).
54. A. T. MALE and V. DEPIERRE, *J. Lub. Technol. Trans. ASME* **92** (1970) 389.
55. Y. SAIDA, C. H. LEE and S. KOBAYASHI, in "Proceedings of the 2nd Inter-American Conference on Materials Technology" (Mexico, 1970) p. 108.
56. V. NAGPAL, G. D. LAHOTI and T. ALTAN, *J. Engng Ind. Trans. ASME* **100** (1978) 413.
57. J. F. ALDER and V. A. PHILLIPS, *J. Inst. Met.* **83** (1954–55) 80.
58. J. A. BAILEY and A. R. E. SINGER, *ibid.* **92** (1964–65) 288.
59. V. S. LINDHOM, *J. Mech. Phys. Solids* **12** (1964) 317.
60. G. M. BOUFEN and G. S. PHILLIPS, *Proc. ASTM* **51** (1976) 761.
61. M. MALATYNSKI and J. KLEPACZKO, *Int. J. Mech. Sci.* **22** (1980) 173.
62. R. A. C. SLATER, W. JOHNSON and S. Y. AKU, *ibid.* **10** (1968) 169.
63. A. GHOSH and J. L. DUNCAN, *ibid.* **12** (1970) 499.
64. D. S. FIELDS Jr and T. J. STEWART, *ibid.* **13** (1971) 63.
65. H. NAZIRI and R. PEARCE, *J. Inst. Met.* **10** (1973) 41.
66. K. A. PADMANABHAN, *Trans. Ind. Inst. Met.* **26**(3) (1973) 41.
67. C. M. SELLARS, in "Proceedings of the International Conference", "Hot Working and Forming Processes" (Metals Society, London, 1979) p. 1.
68. A. P. SINGH and K. A. PADMANABHAN, *J. Mater. Sci.* **17** (1982) 821.
69. H. J. E. HAMEL, *J. South African Inst. Min. Met.* **72** (1972) 44.
70. A. P. SINGH and K. A. PADMANABHAN, *J. Mater. Sci.* **26** (1991) 5488.

Received 19 March  
and accepted 20 December 1990